Supplementary Information for

Differential expansion speeds of Indo-Pacific warm pool and deep convection favoring pool under greenhouse warming

Jeremy Cheuk-Hin Leung[1], Banglin Zhang[1,2,3]*, Qiuying Gan[1,4], Lei Wang[4], Weihong Qian[1,5], Zeng-Zhen Hu[6]

[1]Guangzhou Institute of Tropical and Marine Meteorology/Guangdong Provincial Key Laboratory of Regional Numerical Weather Prediction, CMA, Guangzhou, China

[2]College of Atmospheric Science, Lanzhou University, Lanzhou, China

[3]Southern Marine Science and Engineering Guangdong Laboratory, Zhuhai, China

[4]Laboratory for Coastal Ocean Variation and Disaster Prediction, College of Ocean and Meteorology, Guangdong Ocean University, Zhanjiang, China

[5]Department of Atmospheric and Oceanic Sciences, Peking University, Beijing, China

[6]Climate Prediction Center, NCEP/NWS/NOAA, 5830 University Research Court, College Park, MD, 20740, USA

This file includes:

1. Supplementary Figure 1: Increasing SST threshold for IPWP deep convection from 1979–2020.
2. Supplementary Figure 2: Changes in the DCFP and IPWP area in the past four decades.
3. Supplementary Figure 3: Changes in the DCFP and IPWP area in the past four decades, based on different deep convection criteria.
4. Supplementary Figure 4: Changes in the DCFP and IPWP area in the past four decades, based on different deep convection criteria.
5. Supplementary Figure 5: Variability of SST threshold for different deep convection criteria in climate simulations.
6. Supplementary Figure 6: Long-term change of the DCFP size in future climate projections under the SSP1-2.6 scenario.
7. Supplementary Figure 7: Long-term change of the DCFP size in future climate projections under the SSP2-4.5 scenario.
8. Supplementary Figure 8: Long-term change of the DCFP size in future climate projections under the SSP5-8.5 scenario.
9. Supplementary Figure 9: The eovlution of $DCFP_{conv}$ shape from 2015–2100 under the SSP1-2.6 scenario.
10. Supplementary Figure 10: The eovlution of $DCFP_{conv}$ shape from 2015–2100 under the SSP2-4.5 scenario.
11. Supplementary Figure 11: The eovlution of $DCFP_{conv}$ shape from 2015–2100 under the SSP5-8.5 scenario.
12. Supplementary Figure 12: Weakening of the Pacific Walker circulation in model simulation.
13. Supplementary Figure 13: Relationship between σ_{conv} and precipitation over the Indo-Pacific Ocean in model simulations.
14. Supplementary Table 1: Long-term trends of σ_{trop} (unit: °C/decade) in the past and future projected climate change.
15. Supplementary Table 2: Long-term trends of $DCFP_{trop}$ (unit: °C/decade) in the past and future projected climate change.

Supplementary Figures

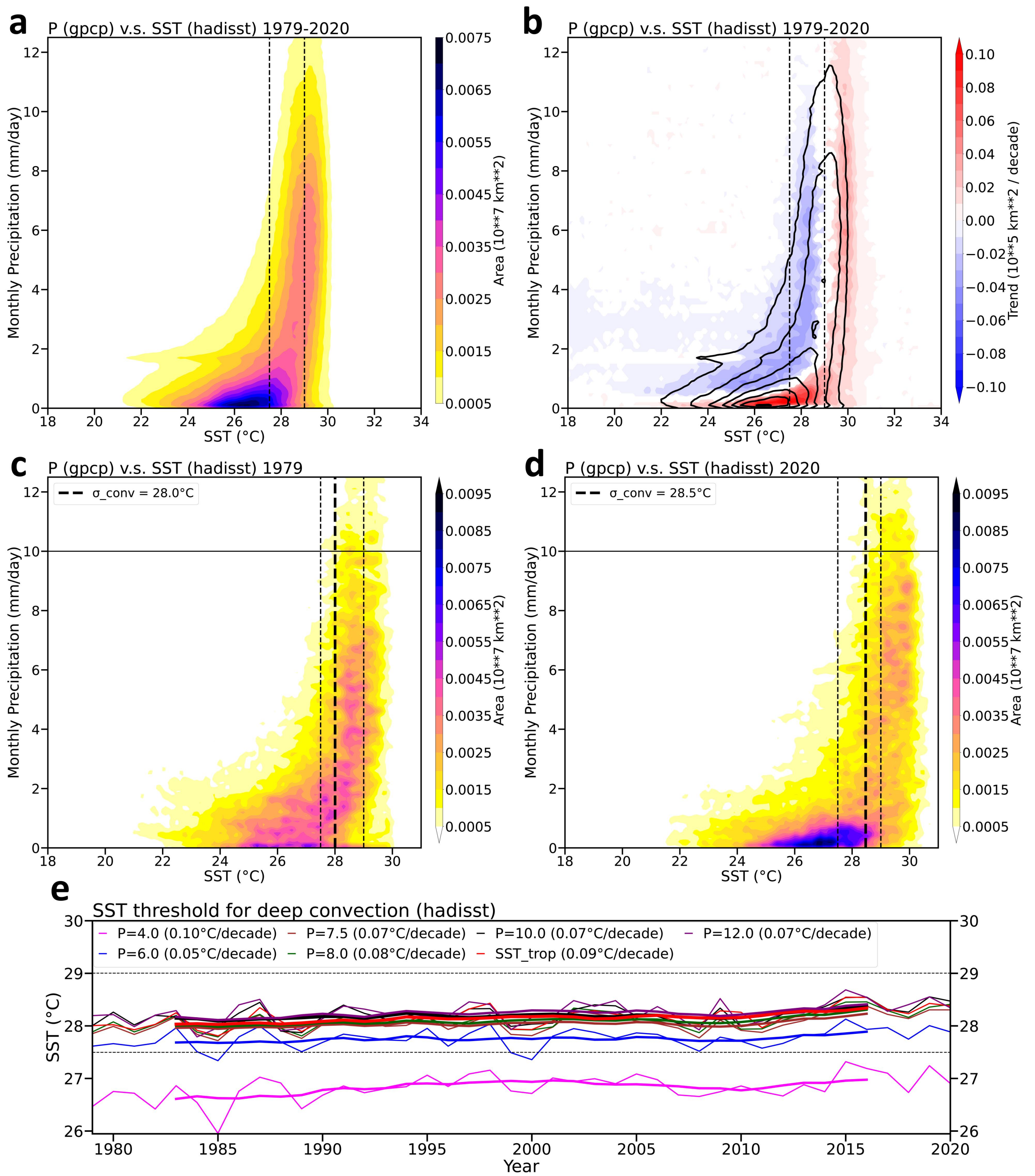

Supplementary Figure 1: Increasing SST threshold for IPWP deep convection from 1979–2020. a, P-SST JFD averaged over 1979–2020 (shading, 0.05×10^5 km^2 interval). **b,** Long-term mean (same as (**a**), contour, 0.1×10^5 km^2 interval) and long-term trend (shading, 0.01×10^5 km^2 interval, only trends being significant at the 90% confidence level are plotted) of the P-SST JFD from 1979–2020. **c–d,** P-SST JFD (shading, 0.05×10^5 km^2 interval) in 1979 (**c**) and 2020 (**d**). The thin vertical dashed lines in (**a–d**) denote 27.5°C and 29.0°C, the common range of IPWP definitions. The thick vertical dashed lines in (**c–d**) denote the estimated σ_{conv} (28.0°C for 1979, and 28.5°C for 2020). **e,** Time series (thin solid lines) of σ_{conv} (unit: °C) derived from different precipitation criteria and σ_{trop} (unit: °C) over the Indo-Pacific Ocean. The thick solid lines denote 9-year running mean series, which filter out the interannual variability. The linear trends of all series, marked on the figure legend, are statistically significant at the 99.9% confidence level. Results are based on the HadISST and GPCP precipitation data. The results are consistent with that shown in Fig. 1, indicating that the observed σ_{conv} is not a fixed value, and has been increasing steadily since 1979.

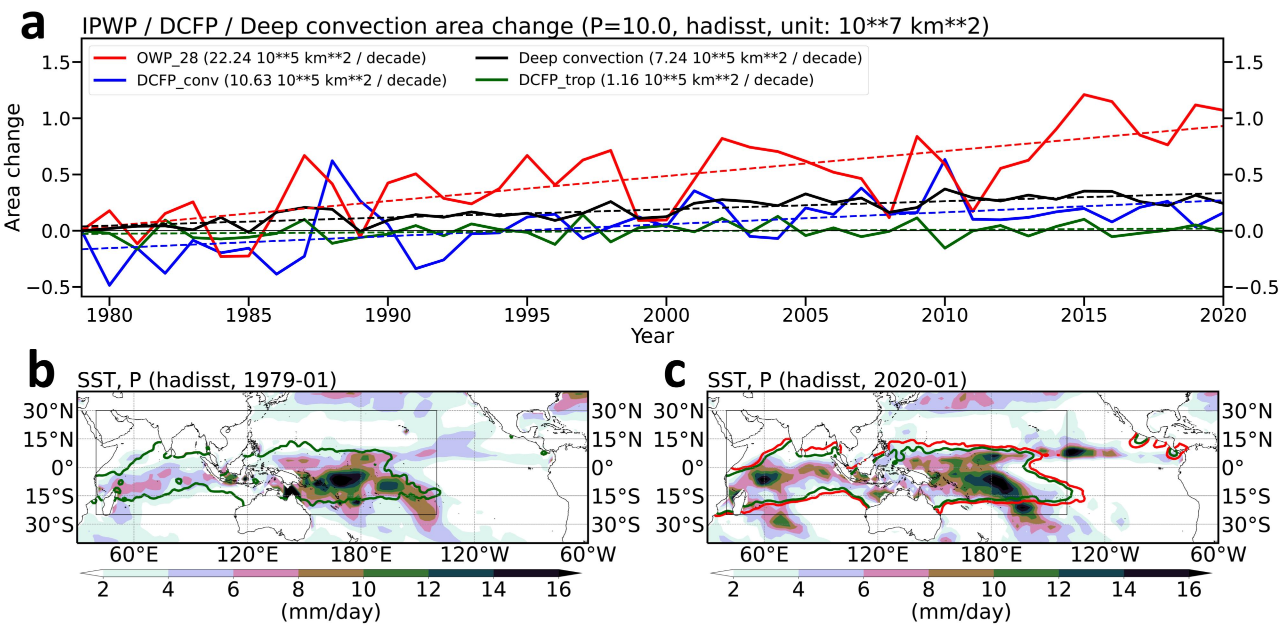

Supplementary Figure 2: Changes in the DCFP and IPWP area in the past four decades. a, Time series of the area change (unit: 10^7 km^2) of OWP_{28} (red line), $DCFP_{conv}$ (blue line), $DCFP_{trop}$ (green line), and that of the area with monthly precipitation rate larger than 10 mm/day (i.e., deep convection area, black line) inside the Indo-Pacific Ocean (25°S–25°N, 40°E–220°E; black box in (**b**) and (**c**)). The linear trends are marked on the figure legend. Trends of all series are statistically significant at the 99.9% confidence level, except that of $DCFP_{trop}$ is statistically insignificant. **b–c,** Monthly precipitation distribution (shading, 2 mm/day interval) in January 1979 (**b**) and January 2020 (**c**), where the red, blue, and green contours respectively indicate the regions covered by the OWP_{28}, $DCFP_{conv}$ (σ_{conv} = 28.0°C for 1979 and 28.5°C for 2020), and $DCFP_{trop}$ (σ_{trop} = 28.0°C for 1979 and 28.4°C for 2020). Results are based on the HadISST and GPCP precipitation data. The results are consistent with those in Fig. 4. As σ_{conv} and σ_{trop} increases, the traditionally defined IPWP may cover a comparatively large region without deep convection.

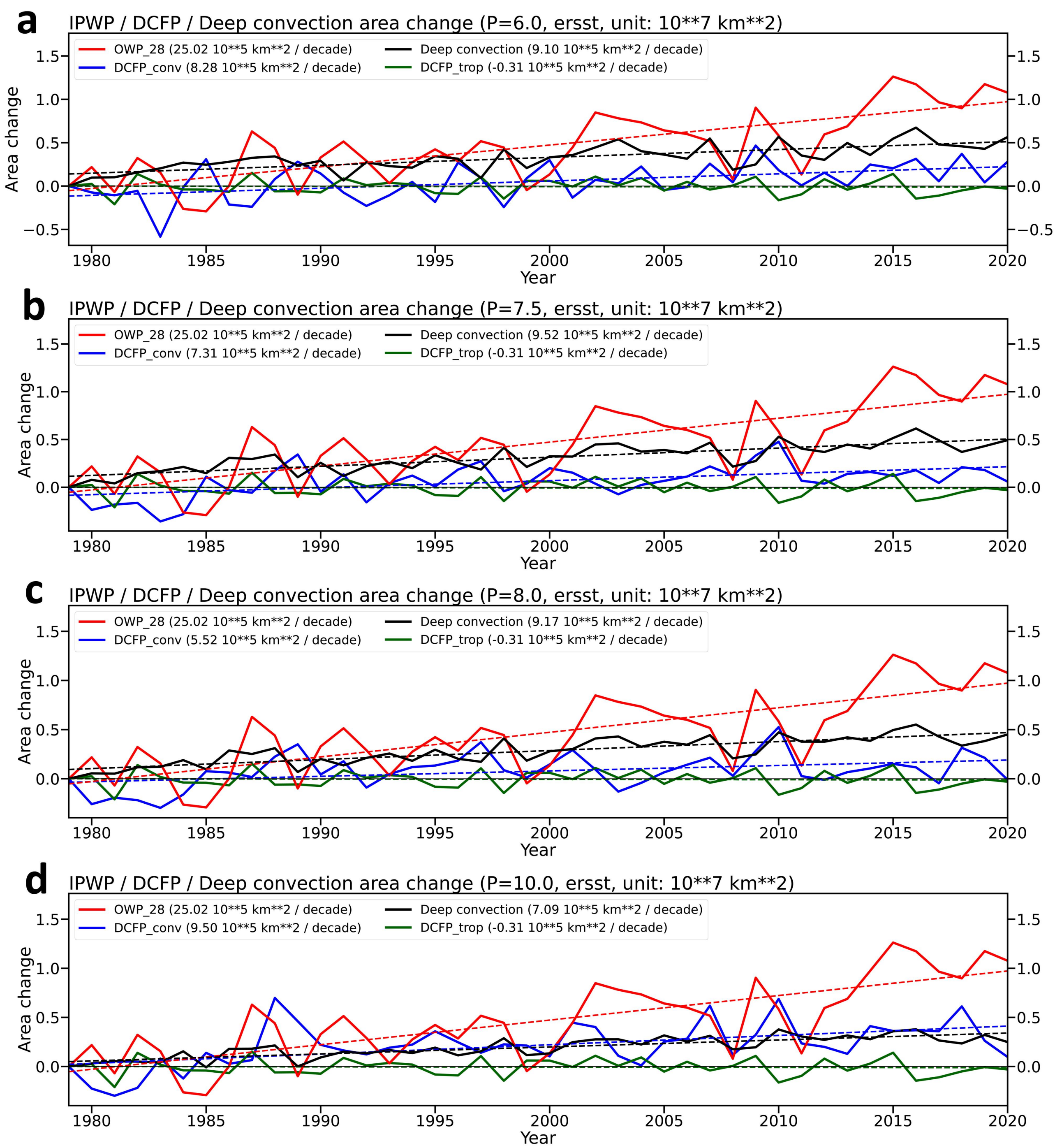

Supplementary Figure 3: Changes in the DCFP and IPWP area in the past four decades, based on different deep convection criteria. a–d, Same as Supplementary Figure 2a, except that the $DCFP_{conv}$ is defined based on different deep convection criteria: P=6.0 mm/day (**a**), P=7.5 mm/day (**b**), P=8.0 mm/day (**c**), P=10.0 mm/day (**d**), respectively. Results are based on ERSSTv5.

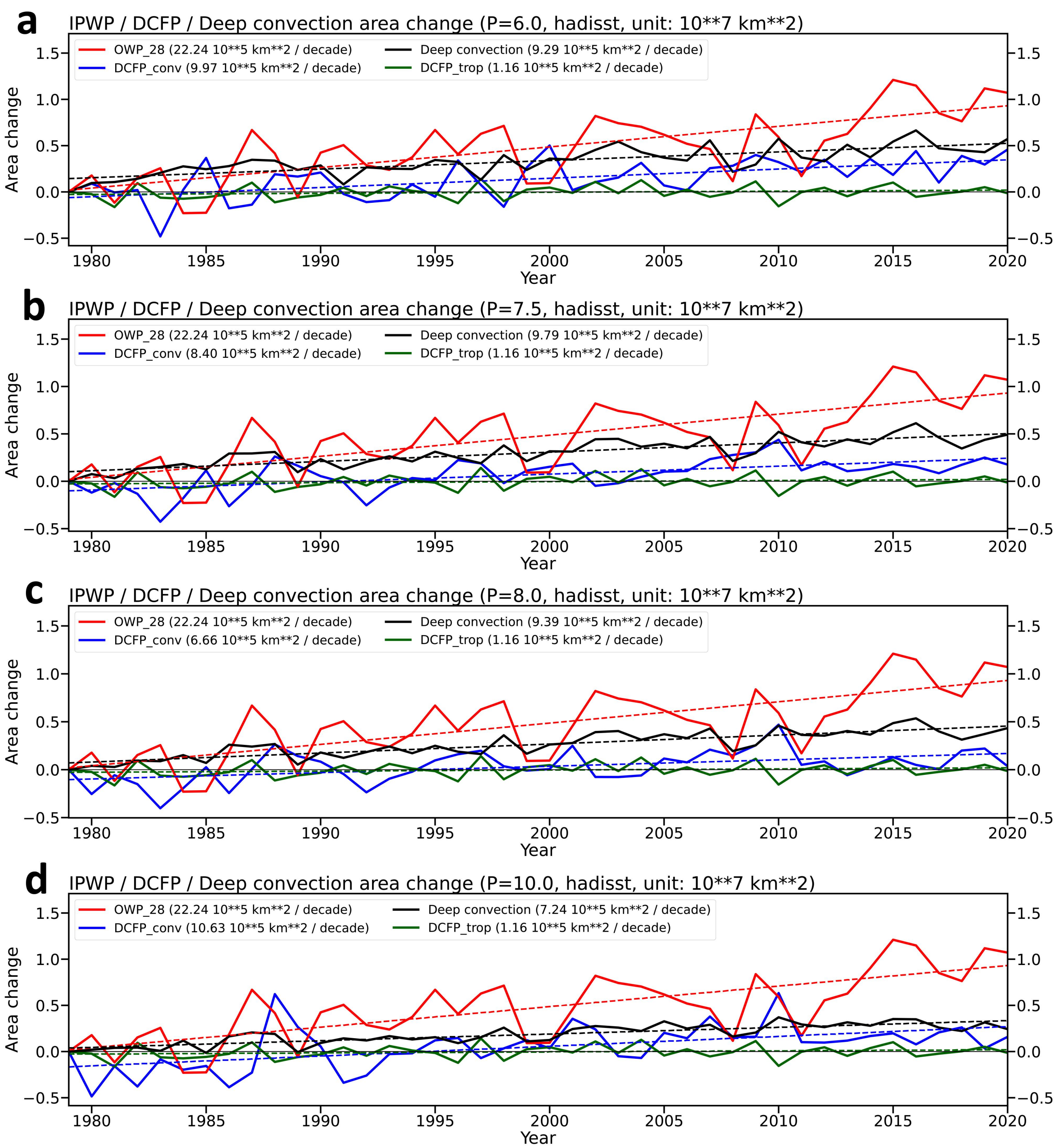

Supplementary Figure 4: Changes in the DCFP and IPWP area in the past four decades, based on different deep convection criteria. a–d, Same as Supplementary Figure 2a, except that the $DCFP_{conv}$ is defined based on different deep convection criteria: P=6.0 mm/day (**a**), P=7.5 mm/day (**b**), P=8.0 mm/day (**c**), P=10.0 mm/day (**d**), respectively. Results are based on HadISST.

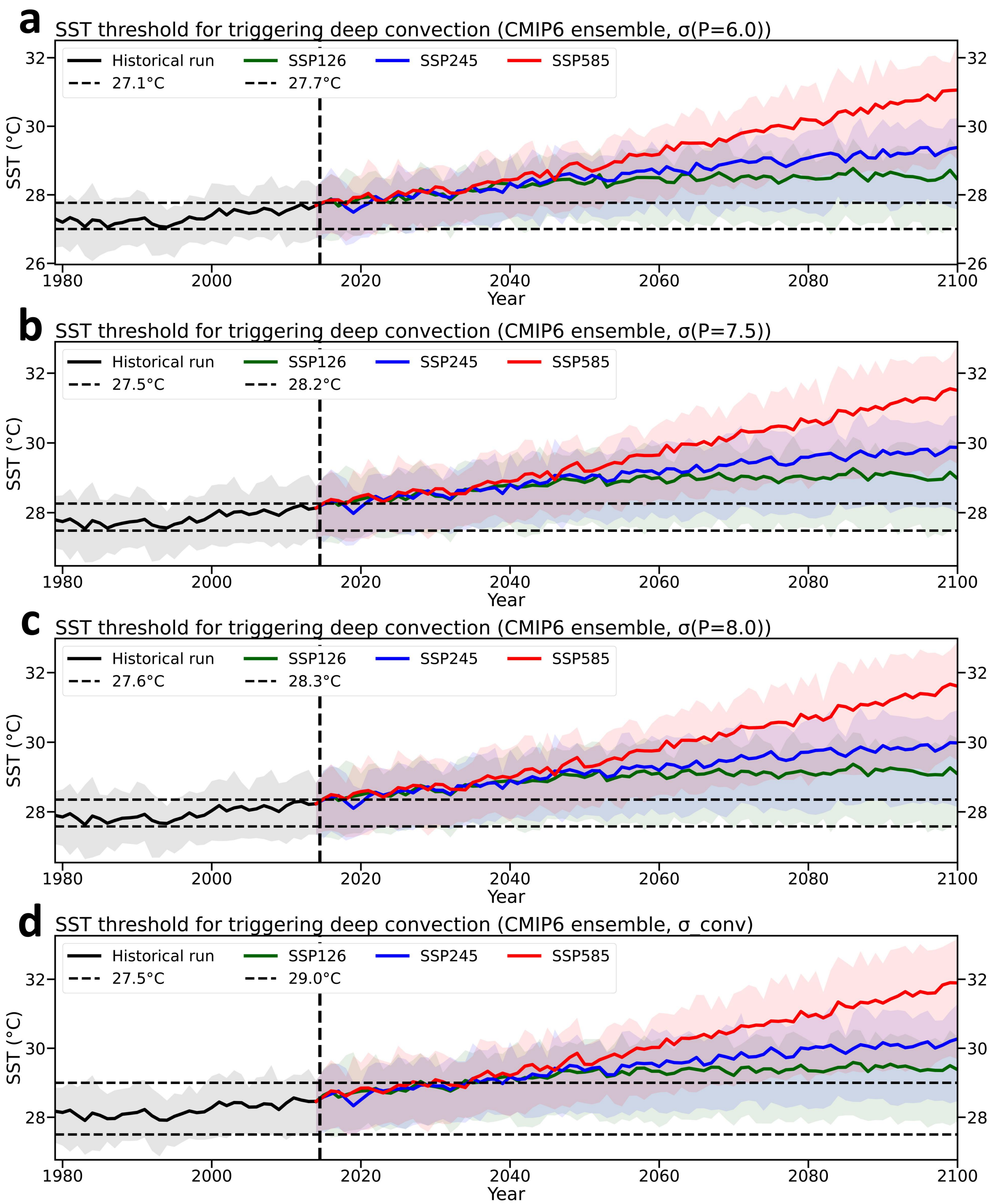

Supplementary Figure 5: Variability of SST threshold for different deep convection criteria in climate simulations. a–d, Time series (unit: °C) of σ_{conv} defined based on different deep convection criteria: P=6.0 mm/day (**a**), P=7.5 mm/day (**b**), P=8.0 mm/day (**c**), P=10.0 mm/day (**d**), respectively. Results are obatined by the five best CMIP6 model under the historical run (black line), SSP1-2.6 (green line), SSP2-4.5 (blue line), and SSP5-8.5 (red line), respectively. Shadings denote the uncertainties of model results.

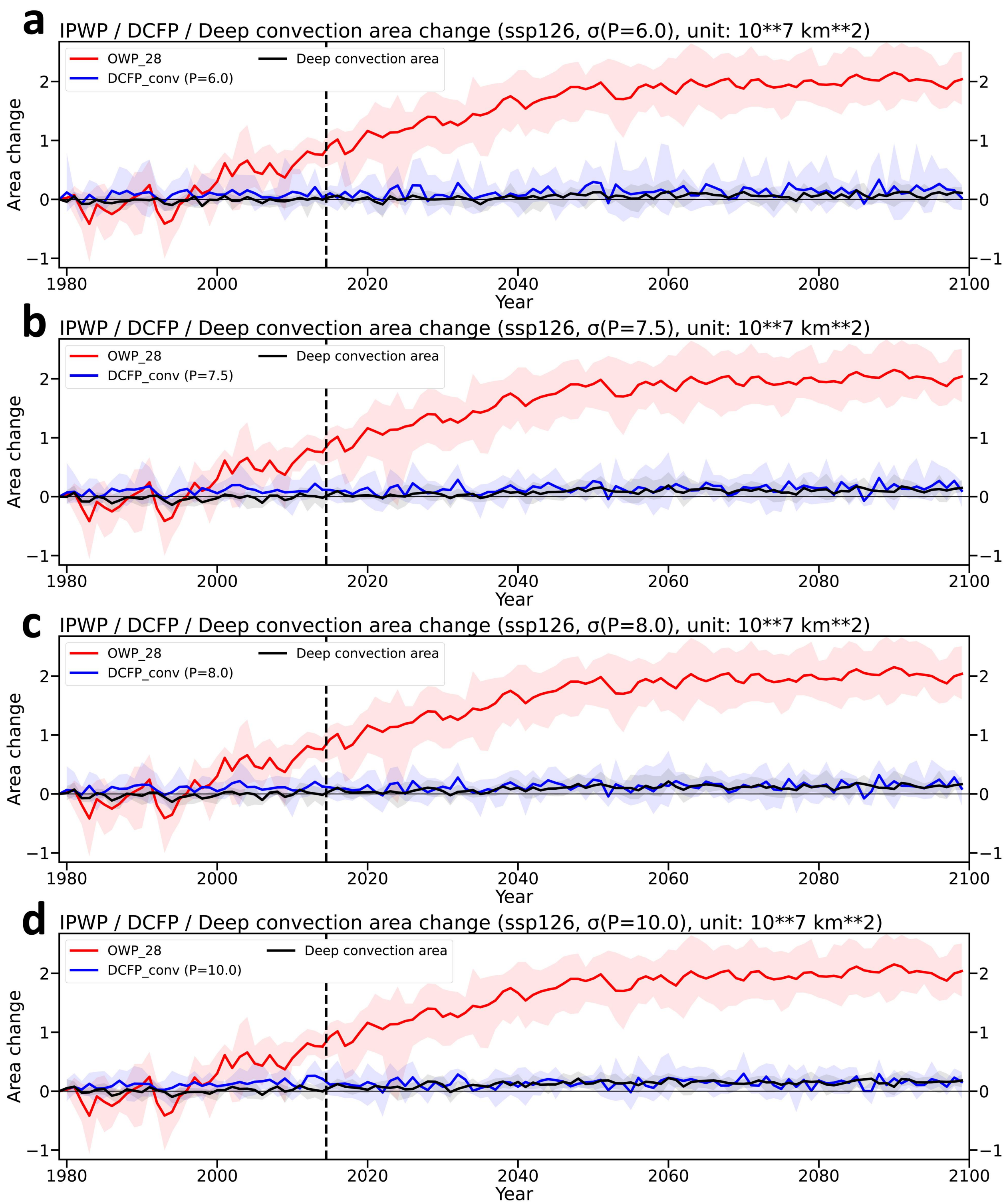

Supplementary Figure 6: Long-term change of the DCFP size in future climate projections under the SSP1-2.6 scenario. **a–d,** Time series of the area change (unit: 10^7 km^2) of the OWP_{28} (red lines), $DCFP_{conv}$ (blue lines), and deep convection (black lines) inside the Indo-Pacific Ocean under the SSP1-2.6 scenario, based on different deep convection criteria:

P=6.0 mm/day (**a**), P=7.5 mm/day (**b**), P=8.0 mm/day (**c**), P=10.0 mm/day (**d**), respectively. Shadings denote the uncertainties of model results. Results are based on the five best CMIP6 models.

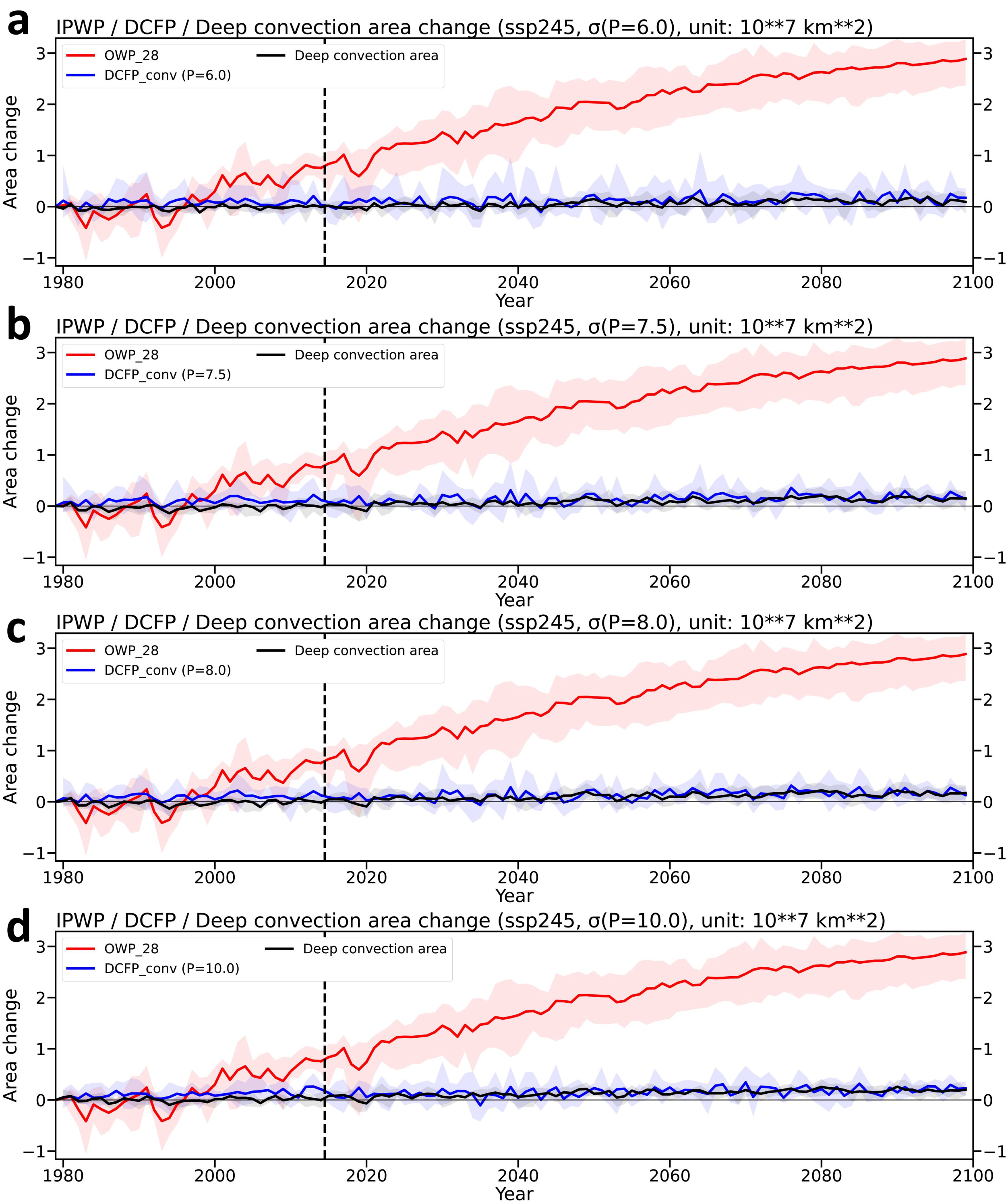

Supplementary Figure 7: Long-term change of the DCFP size in future climate projections under the SSP2-4.5 scenario. **a–d,** Time series of the area change (unit: 10^7 km^2) of the OWP_{28} (red lines), $DCFP_{conv}$ (blue lines), and deep convection (black lines) inside the Indo-Pacific Ocean under the SSP2-4.5 scenario, based on different deep convection criteria:

P=6.0 mm/day (**a**), P=7.5 mm/day (**b**), P=8.0 mm/day (**c**), P=10.0 mm/day (**d**), respectively. Shadings denote the uncertainties of model results. Results are based on the five best CMIP6 models.

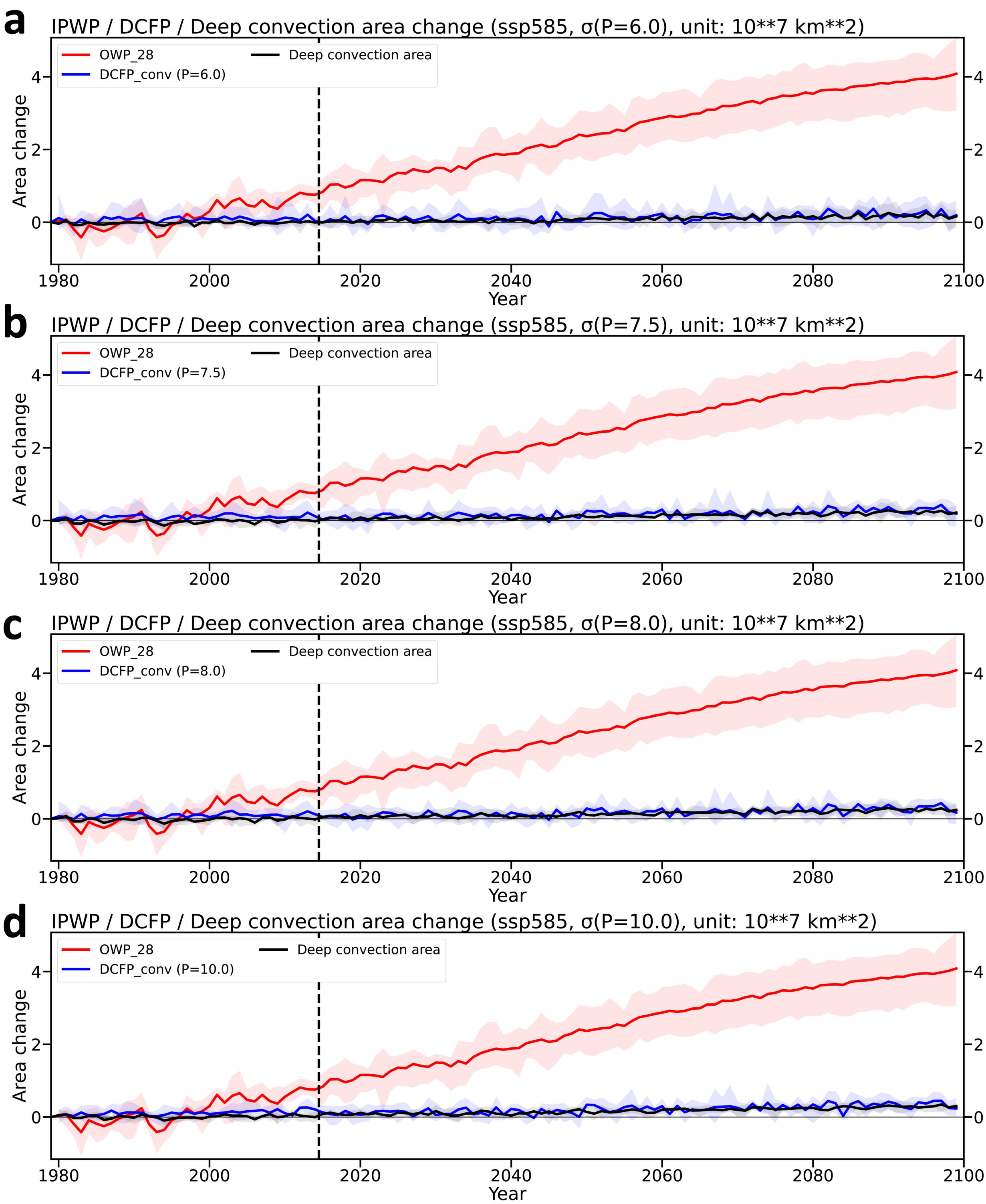

Supplementary Figure 8: Long-term change of the DCFP size in future climate projections under the SSP5-8.5 scenario. **a–d,** Time series of the area change (unit: 10^7 km^2) of the OWP$_{28}$ (red lines), DCFP$_{conv}$ (blue lines), and deep convection (black lines) inside the Indo-Pacific Ocean under the SSP5-8.5 scenario, based on different deep convection criteria:

P=6.0 mm/day (**a**), P=7.5 mm/day (**b**), P=8.0 mm/day (**c**), P=10.0 mm/day (**d**), respectively. Shadings denote the uncertainties of model results. Results are based on the five best CMIP6 models.

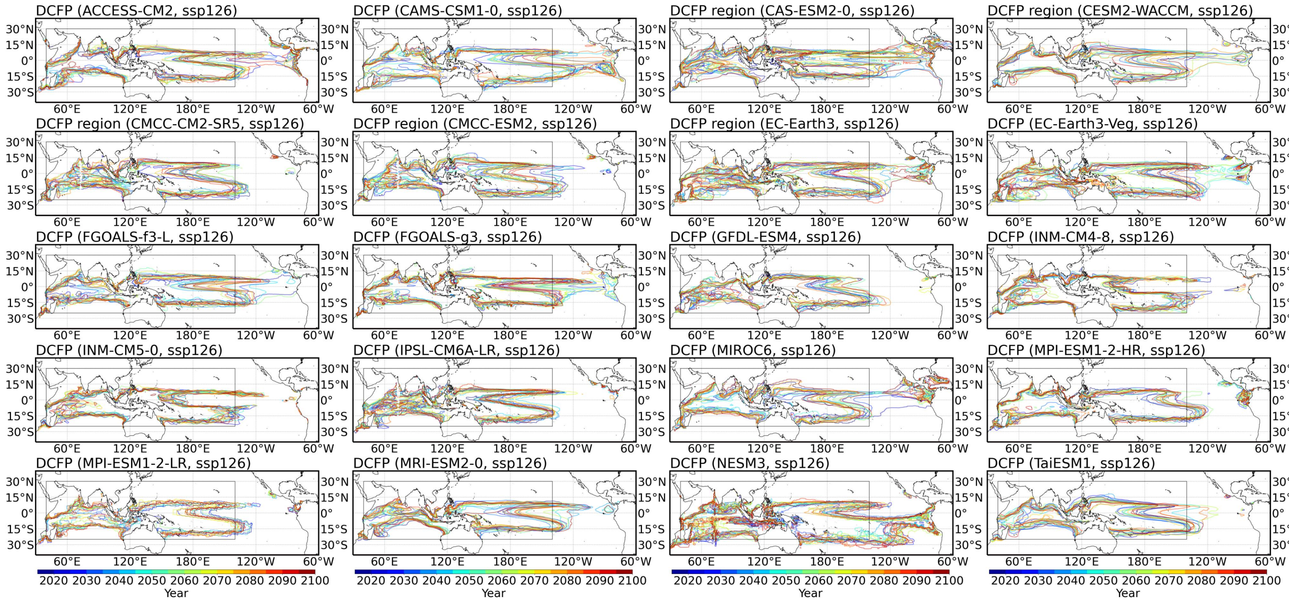

Supplementary Figure 9: The eovlution of $DCFP_{conv}$ shape from 2015–2100 under the SSP1-2.6 scenario. The $DCFP_{conv}$ region of every 5 years from 2015–2100 under the SSP1-2.6 scenario simulated by 20 CMIP6 models.

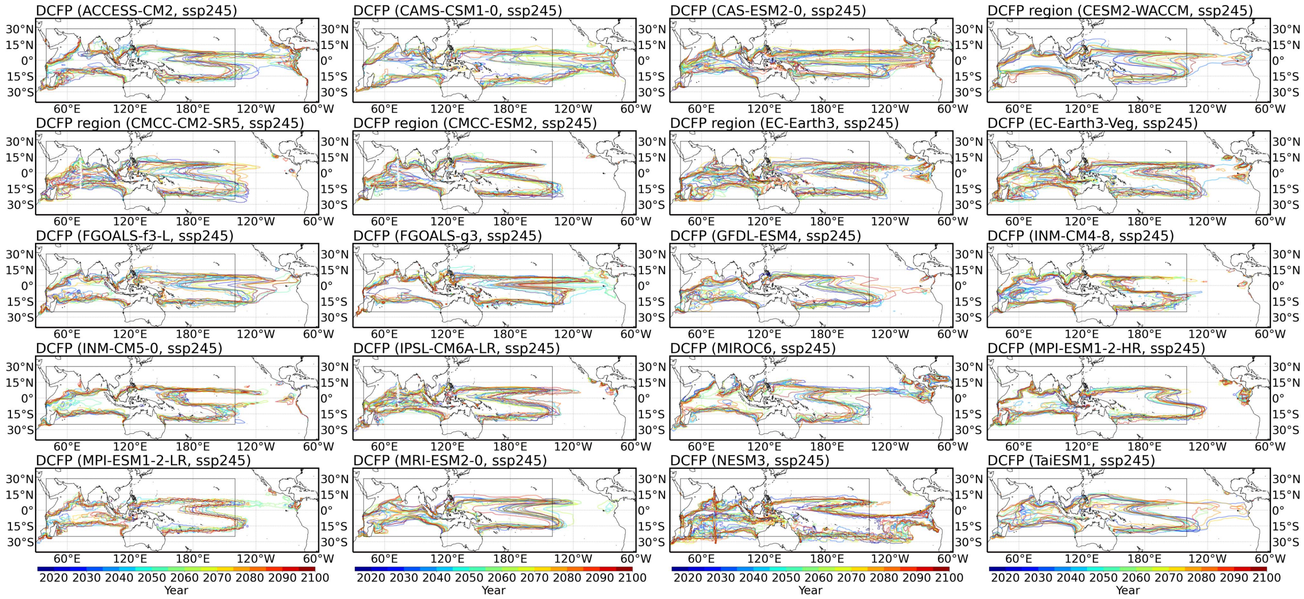

Supplementary Figure 10: The eovlution of $DCFP_{conv}$ shape from 2015–2100 under the SSP2-4.5 scenario. The $DCFP_{conv}$ region of every 5 years from 2015–2100 under the SSP2-4.5 scenario simulated by 20 CMIP6 models.

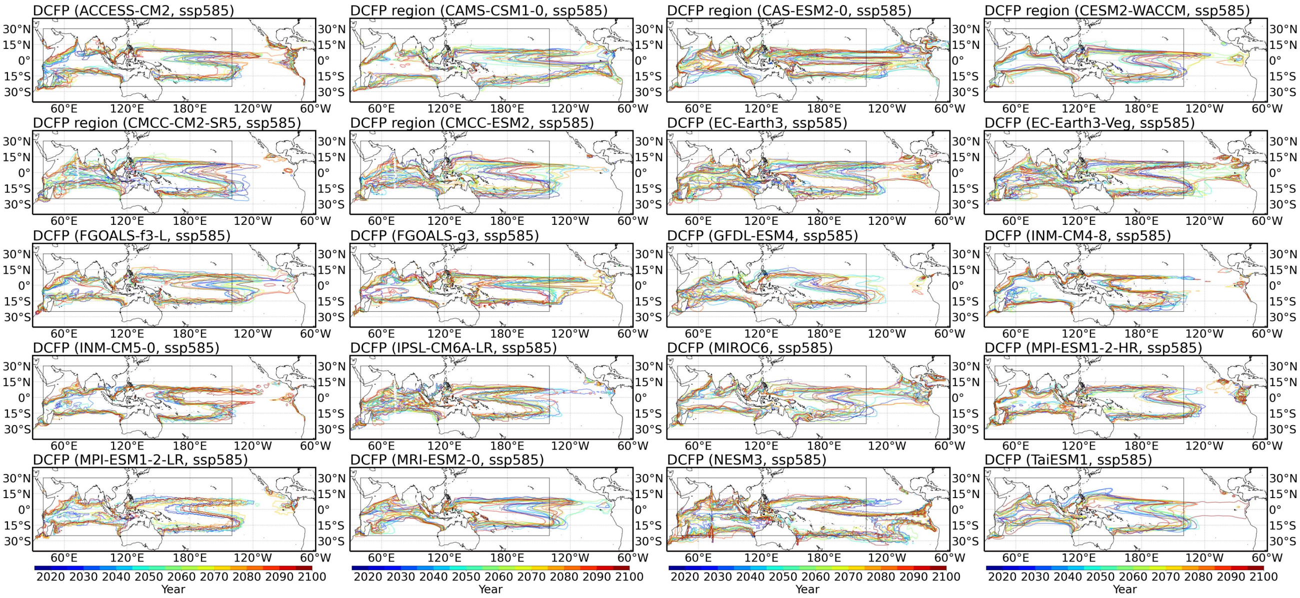

Supplementary Figure 11: The eovlution of $DCFP_{conv}$ shape from 2015–2100 under the SSP5-8.5 scenario. The $DCFP_{conv}$ region of every 5 years from 2015–2100 under the SSP5-8.5 scenario simulated by 20 CMIP6 models.

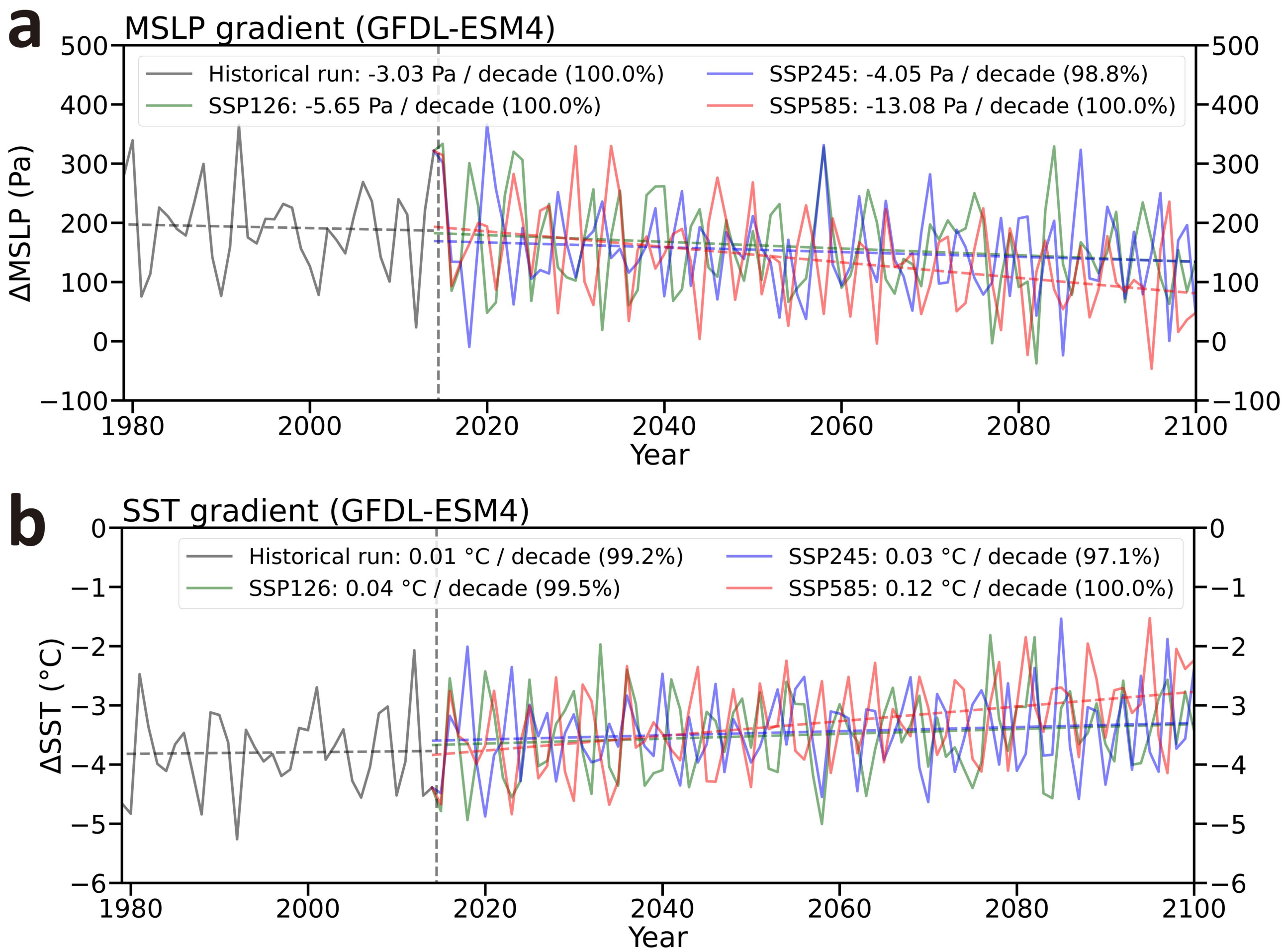

Supplementary Figure 12: Weakening of the Pacific Walker circulation in model simulation. a, Time series of mean sea level differences (∆MSLP) (units: Pa) between equatorial central/eastern Pacific (5°S–5°N, 200°–280°E) and the Indian Ocean/western Pacific (5°S–5°N, 80°–160°E), simulated by the GFDL-ESM4 model under the historical run (black line), SSP1-2.6 (green line), SSP2-4.5 (blue line), and SSP5-8.5 (red line), respectively**. b,** Same as (**a**), except for the SST difference (ΔSST) (units: °C) between equatorial central/eastern Pacific (5°S–5°N, 200°–280°E) and the Indian Ocean/western Pacific (5°S–5°N, 80°–160°E). The linear trends of all series are marked on the figure legend. Results are based on the simulation results of the GFDL model. The figure shows the weakening trends of the Pacific Walker circulation in the future climate projection under different emission scenarios.

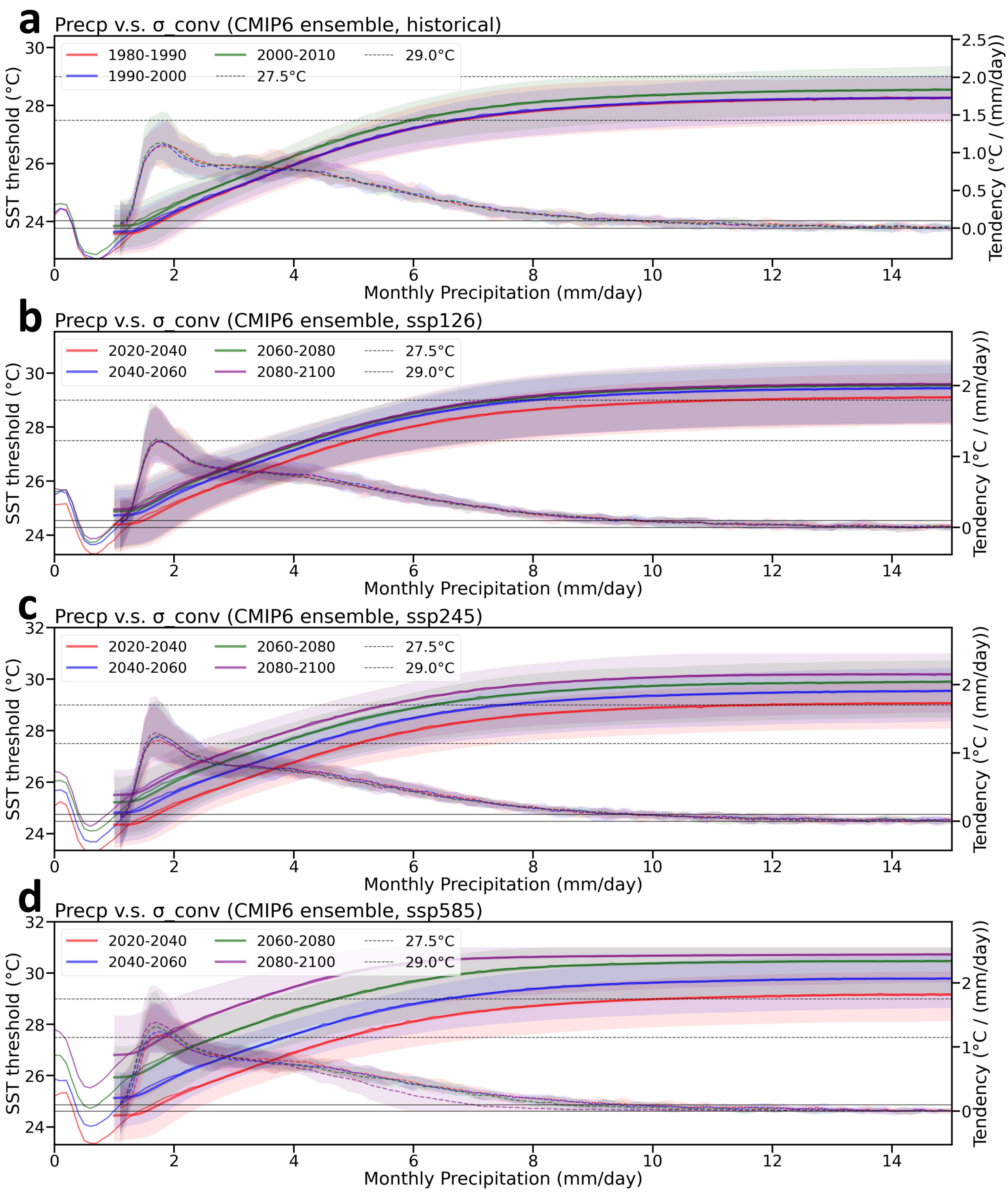

Supplementary Figure 13: Relationship between σ_{conv} and precipitation over the Indo-Pacific Ocean in model simulations. a, Curve (thin solid lines) of ensemble σ_{conv} (unit: °C) against precipitation (unit: mm/day) averaged over 1980–1990 (red), 1990–2000 (blue), 2000–2010 (green), based on the historical runs of the five best CMIP6 models. **b–d,** Curve (thin solid lines) of ensemble σ_{conv} (unit: °C) against precipitation (unit: mm/day) averaged over 2020–2040 (red), 2040–2060 (blue), 2060–2080 (green), and 2080–2100 (green), under the **(b)** SSP1-2.6, **(c)** SSP2-4.5, and **(d)** SSP5-8.5 scenarios based on the five best CMIP6 models. The thick solid lines are the 21-point running mean filtered curve of the thin solid lines, which are equivalent to the 21-point running mean filtered 20% contour lines of JCFD (thick solid lines in Fig. 2). The dashed lines are the slope (first derivative, unit: °C/(mm/day)) of the 21-point running mean filtered curves. The thin horizontal black dashed lines denote 27.5°C and 29.0°C, the common range of IPWP definitions. The results show that while the σ_{conv} slightly shifts upward through greenhouse warming, the relationship between σ_{conv} and precipitation does not exhibit significant changes.

Supplementary Table 1. Long-term trends of σ_{trop} (unit: °C/decade) in the past and future projected climate change, based on ERSSTv5, HadISST, and 20 CMIP6 models. Bold texts denote the five models that could better capture the historical $DCFP_{conv}$ area trend. All trends are statistically significant at the 99.9% confidence level, except those marked with asterisks.

Observation / Models	1979–2020	1979–2014	2015–2100 (SSP1-2.6)	2015–2100 (SSP2-4.5)	2015–2100 (SSP5-8.5)
ERSSTv5	0.11	0.07	/	/	/
HadISST	0.09	0.09	/	/	/
CMIP6 Ensemble	/	0.15	0.07	0.18	0.37
CMIP6 Best	/	0.13	0.09	0.21	0.41
ACCESS-CM2	**/**	**0.14**	**0.12**	**0.23**	**0.48**
CAMS-CSM1-0	/	0.10	0.04	0.12	0.24
CAS-ESM2-0	**/**	**0.16**	**0.12**	**0.23**	**0.41**
CESM2-WACCM	**/**	**0.13**	**0.10**	**0.23**	**0.49**
CMCC-CM2-SR5	**/**	**0.10**	**0.11**	**0.22**	**0.40**
CMCC-ESM2	/	0.15	0.15	0.24	0.43
EC-Earth3	/	0.23	0.07	0.19	0.43
EC-Earth3-Veg	/	0.16	0.07	0.19	0.44
FGOALS-f3-L	/	0.17	0.03	0.14	0.32
FGOALS-g3	/	0.14	0.00*	0.11	0.27
GFDL-ESM4	/	0.16	0.04	0.13	0.31
INM-CM4-8	/	0.15	0.02	0.12	0.28
INM-CM5-0	**/**	**0.15**	**0.02**	**0.11**	**0.26**
IPSL-CM6A-LR	/	0.20	0.07	0.23	0.50
MIROC6	/	0.17	0.06	0.14	0.31
MPI-ESM1-2-HR	/	0.12	0.03	0.14	0.29
MPI-ESM1-2-LR	/	0.11	0.03	0.13	0.30
MRI-ESM2-0	/	0.09	0.07	0.18	0.36
NESM3	/	0.19	0.06	0.16	0.38
TaiESM1	/	0.17	0.15	0.26	0.45

Supplementary Table 2. Long-term trends of $DCFP_{trop}$ (unit: °C/decade) in the past and future projected climate change, based on ERSSTv5, HadISST, and 20 CMIP6 models. Bold texts denote the five models that could better capture the historical $DCFP_{conv}$ area trend. All trends are statistically significant at the 99.9% confidence level, except those marked with asterisks.

Observation / Models	1979–2020	1979–2014	2015–2100 (SSP1-2.6)	2015–2100 (SSP2-4.5)	2015–2100 (SSP5-8.5)
ERSSTv5	-0.31*	0.43*	/	/	/
HadISST	1.16*	1.39*	/	/	/
CMIP6 Ensemble	/	1.44*	0.00*	0.16*	1.11
CMIP6 Best	/	3.57	0.00*	-0.37*	0.05*
ACCESS-CM2	**/**	**2.18***	**-0.17***	**-1.34***	**1.70**
CAMS-CSM1-0	/	0.87*	0.58*	-1.05*	2.35
CAS-ESM2-0	**/**	**2.83***	**-0.18***	**-0.28***	**1.32***
CESM2-WACCM	**/**	**3.73***	**-2.22**	**-2.46**	**-4.43**
CMCC-CM2-SR5	**/**	**7.94***	**2.57**	**2.36**	**1.82***
CMCC-ESM2	/	-0.05*	-0.38*	1.92*	1.69*
EC-Earth3	/	1.30*	-1.06*	0.91*	0.51*
EC-Earth3-Veg	/	1.25*	-0.40*	0.70*	1.14*
FGOALS-f3-L	/	-0.16*	0.84*	0.80*	3.79
FGOALS-g3	/	0.22*	0.84*	-0.68*	0.26*
GFDL-ESM4	/	0.39*	-0.66*	-0.33*	-0.36*
INM-CM4-8	/	-1.84*	0.00*	-1.02	-1.23
INM-CM5-0	**/**	**1.78***	**0.14***	**-0.13***	**-0.14***
IPSL-CM6A-LR	/	1.92*	0.58*	2.03	4.75
MIROC6	/	-5.43	0.67*	0.09*	-1.14*
MPI-ESM1-2-HR	/	1.92*	0.37*	0.01*	2.22
MPI-ESM1-2-LR	/	2.60*	0.65*	1.54	2.41
MRI-ESM2-0	/	2.64*	-1.16*	-0.51*	1.96
NESM3	/	1.60*	0.22*	1.11*	3.07
TaiESM1	/	3.62*	-1.57*	-0.50*	0.45*